Structural Characterization of Iron–Bleomycin by Resonance Raman Spectroscopy†

Satoshi Takahashi,‡ Joseph W. Sam,§ Jack Peisach,§,∥ and Denis L. Rousseau*,‡

Contribution from AT&T Bell Laboratories, Murray Hill, New Jersey 07974, and Departments of Molecular Pharmacology and Physiology and Biophysics, Albert Einstein College of Medicine, Bronx, New York 10461

Received December 27, 1993®

Abstract: Resonance enhanced modes in the Raman spectra of the ferric, ferrous, and CO-bound ferrous forms of iron bleomycin A_2 (Fe–BLM) have been detected. Lines in the high-frequency region of the spectrum of the ferric complex are assigned to the amide I (1608 cm^{-1}) and amide II (1478 cm^{-1}) modes of the β-hydroxyhistidine amide moiety. Two other lines in the spectrum (1388 and 1371 cm^{-1}) are assigned to modes of the pyrimidine ring. All of these modes are sensitive to the redox state of the iron and the presence of exogenous ligands. The data indicate that the nitrogen atom of the β-hydroxyhistidine amide and N1 of the pyrimidine ring are two of the ligands that coordinate iron. The valence- and ligand-dependent frequency changes of the amide I mode are similar to the valence- and ligand-dependent changes in the ν_4 mode of iron porphyrins. This suggests the involvement of a delocalized π-electron system in Fe–BLM analogous to that in iron porphyrins. The first experimental evidence for hydroxide ligation to iron in Fe(III)–BLM is demonstrated by the presence of an Fe–OH stretching mode at 561 cm^{-1}. The C–O and the Fe–CO stretching modes of CO–Fe(II)–BLM are located at 1980 and 511 cm^{-1}, respectively. The frequencies of these modes, which are typical of those for iron porphyrin and heme protein CO complexes, indicate that the electronic properties of CO–Fe(II)–BLM are similar to those of CO-bound iron porphyrins.

Introduction

Bleomycin A_2[1,2] (BLM, Figure 1A) is a member of the bleomycin family of glycopeptide antibiotics currently used in the treatment of various neoplasms.[3] While the mechanism of the drug's antitumor effect remains unknown, it has been shown that bleomycin is able to bind transition metal ions, activate oxygen, and specifically cleave DNA and RNA.[4–7] Furthermore, the iron complex of the drug (Fe–BLM), despite its lack of a heme prosthetic group, resembles several hemoproteins in its ability to activate oxygen and in its EPR and Mössbauer spectroscopic properties.[8,9] Knowledge of the local environment of the metal site in Fe–BLM is central to understanding this spectral similarity as well as the drug's mechanism of oxygen activation.

Unfortunately, there is a dearth of direct evidence concerning the ligands which coordinate to the metal in Fe–BLM. Sugiura[10] has proposed that Fe(III)–BLM has octahedral geometry with the β-aminoalanyl secondary amine, pyrimidine, β-hydroxyhistidinyl amide, and imidazole nitrogen atoms bound equatorially and the β-aminoalanyl primary amine and hydroxide as axial ligands, as illustrated in Figure 1B. On the other hand, two structures have been proposed on the basis of NMR studies. Oppenheimer et al.[11] suggest that for the carbon monoxy–ferrous form of the drug (CO–Fe(II)–BLM) the pyrimidine, imidazole, and both β-aminoalanyl amine nitrogen atoms are equatorial ligands and the mannosyl carbamyl group is bound axially. In contrast, Akkerman et al.[12] contend that CO–Fe(II)–BLM has the secondary amine, pyrimidine, β-hydroxyhistidinyl amide, and imidazole nitrogen atoms as equatorial ligands and the sugar carbamyl group bound axially. Thus, there is general agreement that the secondary amine, pyrimidine, and imidazole are equatorial ligands to the iron, while the identities of the fourth equatorial and axial ligands have yet to be elucidated.

Resonance Raman spectroscopy has proven extremely powerful in probing the metal sites of heme and non-heme iron systems. However, although nonresonance Raman spectra have been reported,[13,14] there have been no reports of resonance-enhanced modes from metal–BLM complexes. A strength of resonance Raman spectroscopy is that the modes which show resonance enhancement are, by definition, associated with the excited chromophore.[15] Thus, identification of the modes enhanced by excitation of a transition centered on the iron atom in Fe–BLM would be expected to provide information concerning the coordination of the metal in these species. In this article we report the first demonstration of resonance-enhanced Raman scattering by Fe–BLM in the ferric, ferrous, and CO-ligated

† The portion of this investigation carried out at the Albert Einstein College of Medicine was supported in part by Grants RR02583 and GM40168 from the United States Public Health Service; J.W.S. is supported by Grant T32 GM07288 from the NIGMS; S.T. is supported by Grant GM48714 from the NIGMS.

‡ AT&T Bell Laboratories.

§ Department of Molecular Pharmacology, Albert Einstein College of Medicine.

∥ Department of Physiology and Biophysics, Albert Einstein College of Medicine.

® Abstract published in *Advance ACS Abstracts*, April 1, 1994.

(1) Stubbe, J.; Kozarich, J. W. *Chem. Rev.* **1987**, *87*, 1107–1136.

(2) Petering, D. H.; Byrnes, R. W.; Antholine, W. E. *Chem.-Biol. Interact.* **1990**, *73*, 133–182.

(3) Carter, S. K. In *Bleomycin Chemotherapy*; Sikic, B. I., Rozencweig, M., Carter, S. K., Eds.; Academic Press: New York, 1985; pp 3–35.

(4) Sausville, E. A.; Peisach, J.; Horwitz, S. B. *Biochemistry* **1978**, *17*, 2740–2746.

(5) Suzuki, H.; Nagai, K.; Yamaki, H.; Tanaka, N.; Umezawa, H. *J. Antibiot.* **1969**, *22*, 446–448.

(6) Magliozzo, R. S.; Peisach, J.; Ciriolo, M. R. *Mol. Pharmacol.* **1989**, *35*, 428–432.

(7) Carter, B. J.; De Vroom, E.; Long, E. C.; van der Marel, G. A.; van Boom, J. H.; Hecht, S. M. *Proc. Natl. Acad. Sci. U.S.A.* **1990**, *87*, 9373–9377.

(8) Burger, R. M.; Kent, T. A.; Horwitz, S. B.; Münck, E.; Peisach, J. *J. Biol. Chem.* **1983**, *258*, 1559–1564.

(9) Sligar, S. G.; Murray, R. I. In *Cytochrome P-450, Structure Mechanism, and Biochemistry*; Ortiz de Montellano, P. R., Ed.; Plenum Press: New York 1986; pp 479–503.

(10) Sugiura, Y. *J. Am. Chem. Soc.* **1980**, *102*, 5208–5215.

(11) Oppenheimer, N. J.; Rodriguez, L. O.; Hecht, S. M. *Proc. Natl. Acad. Sci. U.S.A.* **1979**, *76*, 5616–5620.

(12) Akkerman, M. A. J.; Neijman, E. W. J. F.; Wijmenga, S. S.; Hilbers, C. W.; Bermel, W. *J. Am. Chem. Soc.* **1990**, *112*, 7462–7474.

(13) Fairclough, D. P.; Fawcett, V.; Long, D. A.; Taylor, L. H.; Turner, R. L. *Proc. Int. Conf. Raman Spectrosc.* **1978**, *6*, 90–91.

(14) Freeman, T. B.; Santillo, F. S.; Zimba, C. G.; Nafie, L. A.; Dabrowiak, J. C. *J. Raman Spectrosc.* **1983**, *14*, 266–270.

(15) Rousseau, D. L.; Ondrias, M. R. In *Optical Techniques in Biological Research*; Rousseau, D. L., Ed.; Academic Press: Orlando, FL, 1984; pp 65–132.

0002-7863/94/1516-4408$04.50/0

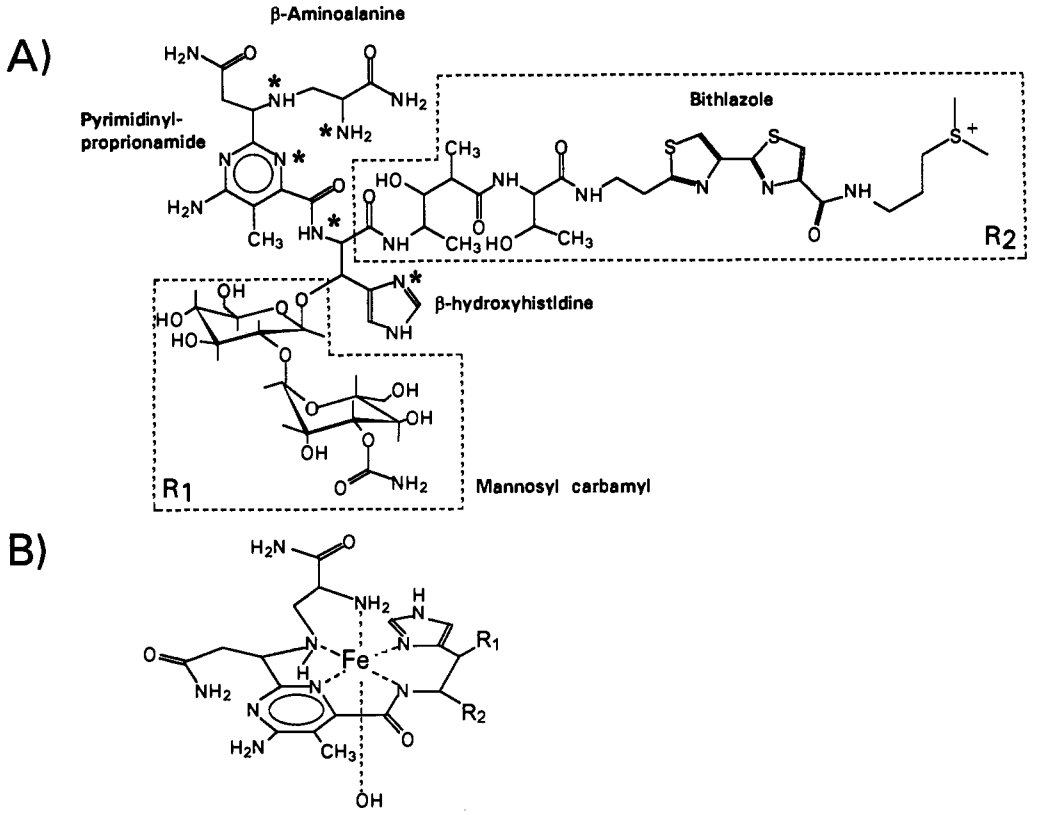

Figure 1. (a) Structure of bleomycin A_2. Asterisks (*) denote proposed ligands in the structure shown in B. (B) Proposed structure of Fe(III)–BLM (adapted from ref 10).

forms. Furthermore, we present evidence for the coordination of OH^- to iron in low-spin ferric BLM and for pyrimidine and the β-hydroxyhistidinyl amide as ligands in all three forms of the metal–drug complex.

Experimental Procedures

Sample Preparation. Bleomycin A_2 was purified from bleomycin sulfate (Blenoxane, the generous gift of Bristol-Myers Co., Syracuse, NY) by FPLC using a mono-S column (Pharmacia, Piscataway, NJ) and a linear 10–50 mM gradient of NH_4HCO_3. Fractions containing bleomycin A_2 were pooled and dried using a speed-vac apparatus (Savant, Farmingdale, NY); their purity was confirmed by TLC according to previously reported methods.[16] The ferric complex of the drug was produced by addition of $Fe^{III}NH_4(SO_4)_2$ to a slight excess of purified BLM followed by at least 10 equiv of Tris buffer to bring the pH to 7.5. Final Fe–BLM concentrations were about 2 mM. Fe(II)–BLM was formed by the anaerobic addition of excess (2–5 equiv) $Na_2S_2O_4$ to a septum-stoppered Raman cell containing Fe(III)–BLM. The CO complex was produced by anaerobically flushing the Raman cell containing Fe(II)–BLM with CO for several minutes. The identity of each sample and its integrity after the Raman measurement were verified by optical spectroscopy[17–20] (SLM-Aminco, Urbana, IL). Isotopically-labeled chemicals were obtained from Aldrich (Milwaukee, WI, D_2O, 99.9%) and ICON (Mt. Marion, NY, $H_2{}^{18}O$, 97%, and $^{13}C^{18}O$, 99%). Final isotope enrichments for BLM solutions in D_2O or $H_2{}^{18}O$ were at least 90%.

Raman Measurements. Excitation laser light was obtained from a krypton ion laser (Spectra Physics, Mountain View, CA). Sample cells at room temperature were rotated at 1000 rpm during the measurements. Rayleigh scattering was removed with a holographic filter (Kaiser, Ann Arbor, MI). Resonance Raman scattered light was dispersed by a single polychromator (SPEX, Metuchen, NJ) equipped with a 1200 groove/mm grating and detected by a cooled CCD camera (Photometrics, Tuscon, AZ). The spectral line width was about 5 cm^{-1}. Typically, several spectra, each acquired for a duration of 3–5 min, were averaged to yield a total accumulation time for each sample of approximately 20 min at 10–30 mW of laser power. Cosmic ray-induced spikes were removed before averaging, and Raman shifts were calibrated using neat indene, acetone, and an aqueous solution of sodium ferrocyanide as frequency standards, providing accuracy of ±2 cm^{-1}.

Results and Discussion

Figure 2 shows the absorption spectra of BLM in the metal-free, ferric-, ferrous-, and carbon monoxy-bound states. The spectrum of metal-free BLM has a broad absorption band centered at 291 nm, which has been assigned to the π–π^* transition of the bithiazole moiety and the n–π^* transition of pyrimidine.[17,18] The binding of iron to the drug results in a red shift of the π–π^* and n–π^* transitions of pyrimidine in the 250- and 300-nm regions, respectively,[17,18] for both oxidation states of the iron. Fe(III)–BLM has transitions at 365 and 384 nm, whereas the ferrous form displays much weaker absorption bands at 370 and 476 nm.[17,19] Binding of carbon monoxide to the reduced form of Fe–BLM yields an absorption spectrum with a band at 384 nm.[20] Although these spectral features have not been assigned, one can speculate that they originate from charge-transfer transitions between iron and its various ligands. Some of these absorptions could also result from iron d–d transitions, but these usually appear in the visible region of the spectrum and have smaller extinction coefficients than the observed lines in the 300–400-nm region.[21] To obtain enhancement from modes of each of the forms of Fe–BLM, we chose 407 nm as the excitation wavelength for the resonance Raman measurements. This excitation wavelength is

(16) Roy, S. N.; Orr, G. A.; Brewer, F.; Horwitz, S. B. *Cancer Res.* **1981**, *41*, 4471–4477.
(17) Dabrowiak, J. C.; Greenaway, F. T.; Santillo, F. S.; Crooke, S. T. *Biochem. Biophys. Res. Commun.* **1979**, *91*, 721–729.
(18) Takita, T.; Muraoka, Y.; Nakatani, T.; Fujii, A.; Iitaka, Y.; Umezawa, H. *J. Antibiot.* **1978**, *31*, 1073–1077.
(19) Burger, R. M.; Horwitz, S. B.; Peisach, J.; Wittenberg, J. B. *J. Biol. Chem.* **1979**, *254*, 12299–12302.
(20) Burger, R. M.; Peisach, J.; Blumberg, W. E.; Horwitz, S. B. *J. Biol. Chem.* **1979**, *254*, 10906–10912.
(21) Cotton, F. A.; Wilkinson, G. *Advanced Inorganic Chemistry*, 4th ed.; Wiley & Sons: London, 1980; pp 619–688.

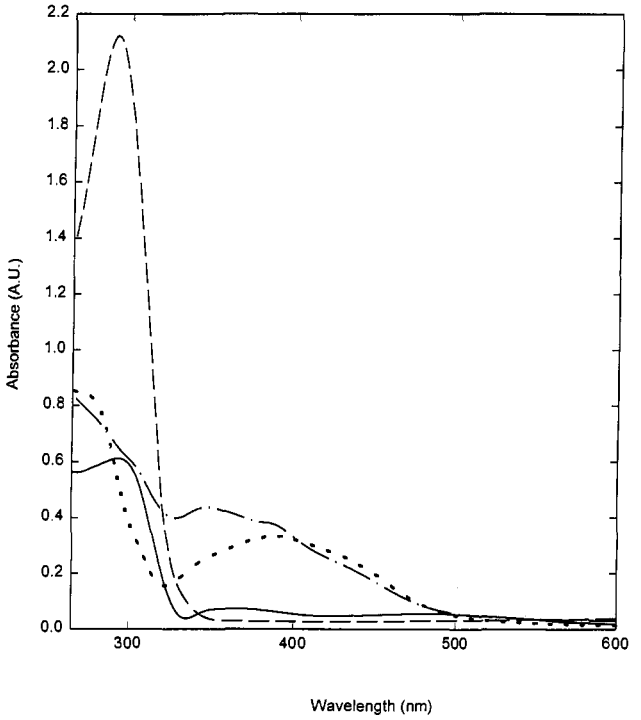

Figure 2. Optical spectra of BLM (– –), CO–Fe(II)–BLM (- - - -), Fe(III)–BLM (– • –), and Fe(II)–BLM (—). The latter three spectra are difference spectra obtaining by substracting the spectrum of metal-free BLM from the spectrum of each complex. Final concentrations were 140 μM BLM, 120 μM Fe, and 5 mM NH_4HCO_3.

beneficial in avoiding fluorescence from the bithiazole and pyrimidine moieties,[22] although we recognize that for the ferrous complex of the drug resonance enhancement will be weak with this excitation.

Metal-free BLM shows little fluorescence with 407-nm excitation even after long laser irradiation; in contrast, upon binding iron, the drug exhibits a fluorescence background which gradually increases with sample age and laser power. The intensity of the fluorescence is higher with 442-nm excitation than with 407-nm excitation. Since there is no apparent change in the optical absorption between freshly complexed and aged samples, the fluorescence does not appear to originate from the Fe–BLM complex itself, but likely from impurities or degradation products caused by photo- or dark reactions of the complex. This fluorescence could be minimized sufficiently to allow Raman measurements by using purified bleomycin A_2, forming the iron–drug complex immediately before performing the spectroscopy, and using moderately low (10–30 mW) excitation laser power. It has been shown that carbon monoxide in CO–Fe(II)–BLM can be photodissociated by visible light irradiation.[23] This was confirmed by our Raman measurements, and accordingly, we used low excitation power (10 mW) to obtain spectra of the CO-bound form.

High-Frequency Region. The high-frequency region (1200–1700 cm^{-1}) of the resonance Raman spectra, obtained with 407-nm excitation, of ferric- (trace A), ferrous- (trace B), and ferrous carbon monoxide-bound (trace C) forms of Fe–BLM is shown in Figure 3. The strongest line in the spectrum at 1540 cm^{-1} is attributed to nonresonant Raman scattering of the bithiazole moiety,[14] which, along with several other weak lines, is observable in the spectra of metal-free BLM (trace D) and the iron-coordinated derivatives. In addition to these nonresonant modes, the spectrum of ferric bleomycin contains several new bands, e.g.

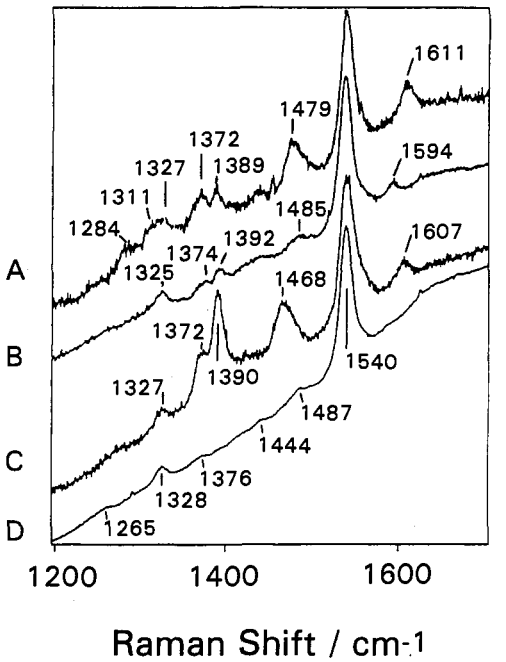

Figure 3. High-frequency region of the resonance Raman spectra of Fe–BLM in H_2O with 407-nm excitation. Traces A, B, C, and D correspond to Fe(III)–BLM, Fe(II)–BLM, CO–Fe(II)–BLM, and metal-free BLM, respectively. No data corrections were performed.

at 1611, 1479, 1389, and 1372 cm^{-1}, which are also observed in the spectra of the ferrous- and ferrous carbon monoxide-bound forms, albeit with varying intensities and frequencies. Since these bands show redox and ligation state dependence and cannot be observed with 521-nm excitation (data not shown), where Fe–BLM displays little optical absorption (Figure 2), we conclude that they are resonance enhanced. Since the presence of nonresonance Raman bands hinders analysis of the resonance Raman bands, the traces in Figure 4 have been corrected to display only the resonance-enhanced modes by subtracting the spectrum of metal-free BLM such that the contribution of the strongest nonresonant line at 1540 cm^{-1} is minimized. Where necessary, a two-point baseline correction was performed to remove any residual fluorescence background. Thus, traces A, B, and C of Figure 4 are the corrected spectra of Fe(III)–BLM, Fe(II)–BLM, and CO–Fe(II)–BLM in H_2O, respectively, whereas traces A′, B′, and C′ correspond to the identical species in D_2O. We have also measured the high-frequency Raman scattering of Fe(III)–, Fe(II)–, and CO–Fe(II)–BLM in $H_2{}^{18}O$, and the spectra (not shown) are identical within experimental error to those of the corresponding samples in $H_2{}^{16}O$.

The features of the Raman spectra in the high-frequency region can be summarized as follows. (1) There are four lines common to the spectra of all three forms (Fe(III), Fe(II), and Fe(II)–CO): two broad lines near 1608 and 1478 cm^{-1} and a narrow doublet at approximately 1388 and 1371 cm^{-1}. All four lines show redox and ligation state dependent frequency and intensity changes but, on the basis of their similarity, can be assumed to arise from the same vibrational mode in each form. The consistency of the deuterium shift patterns, described below, among the three forms is strong support for this argument. (2) Each of the four lines shows a small shift (2–5 cm^{-1}) to higher frequency for samples in D_2O. This implies that the observed modes do not involve movement of an exchangeable proton directly, since such modes show relatively large shifts to lower frequencies upon H/D exchange. In contrast, shifts to higher frequency are usually attributed to hydrogen bonding of the atoms involved in the observed mode or vibrational coupling with another mode having exchangeable protons. (3) The two broad lines at 1608 and 1478 cm^{-1} have similar line widths (for Fe(III)–BLM,

(22) Chien, M.; Grollman, A. P.; Horwitz, S. B. *Biochemistry* **1977**, *16*, 3641–3647.
(23) Sugiura, Y.; Kuwahara, J.; Suzuki, T. *FEBS Lett.* **1985**, *182*, 39–42.

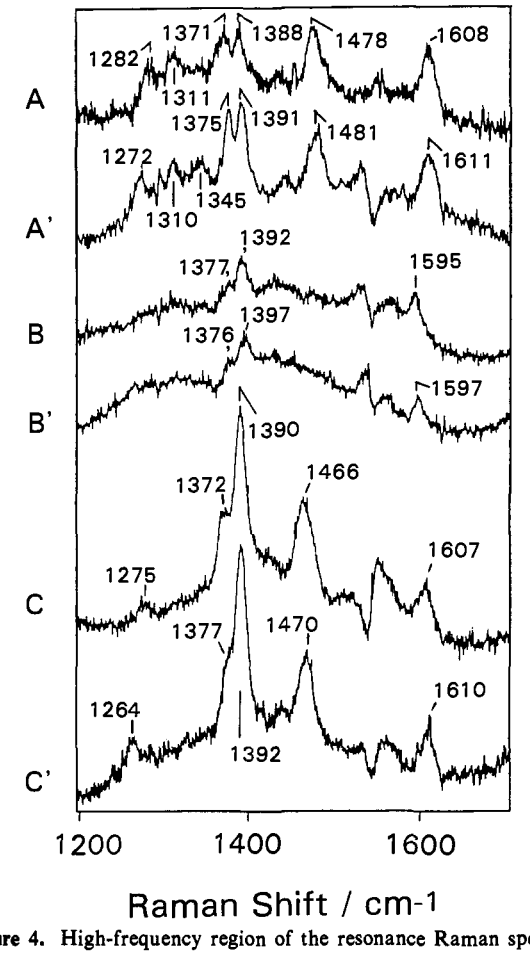

Figure 4. High-frequency region of the resonance Raman spectra of Fe–BLM corrected by subtracting the nonresonant component from the spectra in Figure 3. Linear baseline corrections were performed where necessary. Traces A, B, and C correspond to Fe(III)–BLM, Fe(II)–BLM, and CO–Fe(II)–BLM in H_2O. Traces A′, B′, and C′ correspond to the identical species in D_2O.

both lines have ca. 17 cm^{-1} full width at half-height), and of the four lines, their frequencies are most sensitive to the valency and ligation states of iron. Broad line widths are typical of structural inhomogeneity, so one might envision that these two lines arise from relatively flexible regions of Fe–BLM. (4) The two modes at 1388 and 1371 cm^{-1} which form a doublet pattern have relatively narrow line widths (9- and 12-cm^{-1} full widths at half-height, respectively, for Fe(III)–BLM), and their frequencies are only weakly dependent on the redox state of iron. The 1371-cm^{-1} line displays a larger deuterium shift. (5) There are several weak lines between 1250 and 1350 cm^{-1} that are most apparent in the spectrum of the Fe(III) species and display complicated deuterium shift patterns. Notably, the ratio of the intensity of these lines to that of the 1388-cm^{-1} feature is different between the Fe(III) and Fe(II)–CO states, suggesting that these features arise from a different portion of the BLM molecule than those that give rise to the aforementioned four lines.

In our assignment of the four spectral features in the resonance Raman spectrum, we limited our analysis to the six nitrogen atoms on the bleomycin molecule that previous EPR and NMR spectroscopic investigations have identified as potential ligands to iron in the ferric and CO-bound ferrous complexes.[11,12] These are the primary and secondary amines of the β-aminoalanine residue, N1 of the pyrimidine ring, the imidazole and amide nitrogens of β-hydroxyhistidine, and the mannose carbamyl nitrogen (cf. Figure 1). Of these, the two amines and the carbamyl moiety may be excluded since they have exchangeable protons

Table 1. Frequencies (cm^{-1}) of the Resonance Raman Lines for Fe–BLM and Their Proposed Assignments[a]

proposed assignments	Fe(III)–BLM	Fe(II)–BLM	CO–Fe(II)–BLM
amide I (C=O stretch) of β-hydroxyhistidinyl amide	1608/1611	1595/1597	1607/1610
amide II (C–N stretch) of β-hydroxyhistidinyl amide	1478/1481	not obsd	1466/1470
pyrimidine ring mode	1388/1391	1392/1397	1390/1392
pyrimidine ring mode	1371/1375	1377/1376	1372/1377

[a] The two values of each form correspond to the frequencies for the samples in H_2O and D_2O, respectively.

at their putative coordinated nitrogen atoms, which is inconsistent with the observed deuterium shifts to higher frequency. We also disfavor the assignment of any of the four lines to histidine internal vibrations, since these modes have been shown to exhibit poor resonance enhancement in iron–imidazole complexes.[24] Furthermore, deuterium exchange of free histidine causes a complete change of its nonresonant Raman spectrum.[25,26]

There remain two candidates for ligands to the iron atom to account for the observed resonance-enhanced lines in the Raman spectrum: the amide nitrogen of β-hydroxyhistidine and N1 of the pyrimidine ring. An infrared spectroscopic study of pyridine-2-carboxamide chelates of transition metals demonstrated that the C=O stretching vibration of the amide moiety (amide I mode) is located at 1660 cm^{-1} in the metal-free state and shifts to 1625 cm^{-1} when the amide nitrogen is bound to metal.[27] In addition, Mascharak and co-workers[28–30] observed a similar low-frequency shift with the Cu and Fe complexes of PMAH,[31] a synthetic model of the metal-binding region of bleomycin. The IR spectrum of Fe–PMA has a mode assigned as a carbonyl stretching vibrational of a coordinated amide at 1630 cm^{-1} for the ferric state and 1590 cm^{-1} for the ferrous state.[29] Thus, the absolute frequency and redox state dependence of this mode is remarkably similar to that of the 1608-cm^{-1} line of Fe(III)–BLM, and we are prompted to assign it to the carbonyl stretching vibration of the β-hydroxyhistidinyl amide, Due to the similarity of the 1479-cm^{-1} line to the 1611-cm^{-1} line in line width and redox state dependence, we propose that this feature originates from the C–N stretching vibration (amide II mode) of the coordinated β-hydroxyhistidinyl amide. Furthermore, we propose that the two narrow bands at 1371 and 1388 cm^{-1} arise from pyrimidine internal modes. A previous infrared study of amine-substituted pyrimidine showed that the lines assigned to ring modes were largely deuterium insensitive.[32] Therefore, the assignment of these spectral features as pyrimidine internal modes is consistent with their narrow line widths, low sensitivity to the redox state of iron, and small deuterium shifts. The positions of the high-frequency Raman lines for drug complexes in H_2O and D_2O and their proposed assignments are summarized in Table 1. Lastly, it is important to stress that the absence of mannose carbamyl or β-aminoalanine amine related lines in our results does not necessarily indicate the absence of these groups as ligands.

Low-Frequency Region. Figure 5 shows the low-frequency (300–800 cm^{-1}) spectra of Fe(III)–BLM in $H_2{}^{16}O$ (trace A),

(24) Walters, M. A.; Spiro, T. G. *Inorg. Chem.* **1983**, *22*, 4014–4017.
(25) Ashikawa, I.; Itoh, K. *Biopolymers* **1979**, *18*, 1859–1876.
(26) Harada, I.; Takeuchi, H. In *Spectroscopy of Biological Molecules*; Clark, R. J. H., Hester, R. E., Eds.; Wiley & Sons: London, 1986; pp 113–175.
(27) Sekizaki, M.; Yamasaki, K. *Spectrochim. Acta* **1968**, *25A*, 475–485.
(28) Brown, S. J.; Hudson, S. E.; Stephan, D. W.; Mascharak, P. K. *Inorg. Chem.* **1989**, *28*, 468–477.
(29) Guajardo, R. J.; Hudson, S. E.; Brown, S. J.; Mascharak, P. K. *J. Am. Chem. Soc.* **1993**, *115*, 7971–7977.
(30) Brown, S. J.; Mascharak, P. K.; Stephan, D. W. *J. Am. Chem. Soc.* **1988**, *110*, 1996–1997.
(31) PMAH, in which H is the dissociable amide proton, is the common abbreviation for 2-((*N*-(aminoethyl)amino)methyl)-4-(*N*-(2-(4-imidazoyl)-ethyl)carbamoyl)-5-bromopyrimidine.
(32) Lafaix, A. J.; Lebas, J. M. *Spectrochim. Acta* **1970**, *26A*, 1243–1270.

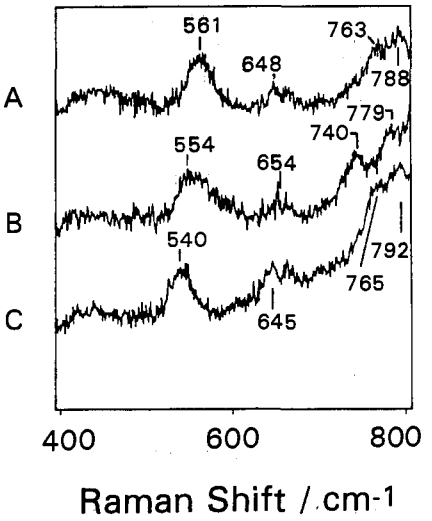

Figure 5. Low-frequency region of the resonance Raman spectra of Fe(III)–BLM in $H_2{}^{16}O$ (A), D_2O (B), and $H_2{}^{18}O$ (C). Linear baseline corrections were performed on the data.

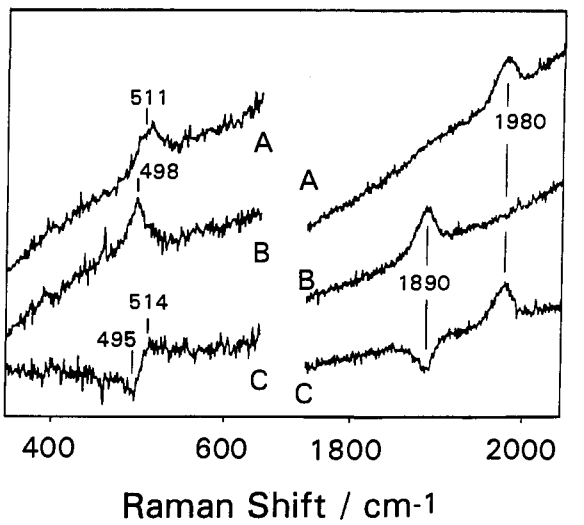

Figure 6. Fe–CO and C–O stretching regions of the resonance Raman spectra of CO–Fe–BLM. Traces A and B were observed for $^{12}C^{16}O$- and $^{13}C^{18}O$-bound Fe(II)–BLM, respectively. Trace C represents their difference spectrum.

D_2O (trace B), and $H_2{}^{18}O$ (trace C); the spectrum of Fe(II)–BLM contains only weak nonresonant modes in this region (data not shown). The line at 561 cm^{-1} in the spectrum of Fe(III)–BLM in $H_2{}^{16}O$ shifts to 554 and 540 cm^{-1} in D_2O and $H_2{}^{18}O$, respectively.[33] The isotope shifts of the 561-cm^{-1} line in both D_2O and $H_2{}^{18}O$ suggest that the mode may involve the motion of a bound water or hydroxide. We are able to exclude an Fe–OH_2 stretching vibration for this mode, since in $[Fe(H_2O)_6]^{2+}$ it occurs at 389 cm^{-1}, which is considerably lower than our value of 561 cm^{-1}.[34] The Fe–OH_2 wagging motion, detected at 575 cm^{-1} for $[Fe(H_2O)_6]^{2+}$, is another candidate for this mode; yet, the observed deuterium shift of 7 cm^{-1} is smaller than one would expect, since the same mode in $[Zn(H_2O)_6]^{2+}$ displays a deuterium shift of 149 cm^{-1}.[34] On the basis of these considerations, we rule out H_2O as the ligand giving rise to these Raman lines. However, the frequency and isotope shift pattern of the 561-cm^{-1} line are consistent with those of a Fe–OH stretching vibration similar to that exhibited by the hydroxide complex of a low-spin ferric heme protein.[35] For example, the Raman spectrum of low-spin ferric myoglobin with bound hydroxide contains an Fe–OH mode at 551 cm^{-1} that shifts by 13 and 22 cm^{-1} in D_2O and $H_2{}^{18}O$, respectively.[36] Thus, we conclude that these results provide the first experimental evidence for the coordination of hydroxide to Fe(III)–BLM, originally hypothesized by Sugiura.[10]

Ferrous Carbon Monoxide-Bound State. Figure 6 shows the C–O and Fe–CO stretching regions of CO–Fe(II)–BLM. Trace A was observed for $^{12}C^{16}O$-bound Fe(II)–BLM and trace B for the $^{13}C^{18}O$-bound form. Trace C is the A–B difference spectrum, showing well-resolved isotope shifts in each region. The lines at 1980 and 511 cm^{-1} can be assigned to C–O stretching and Fe–CO stretching modes, respectively. The C–O stretching frequency we observe is slightly higher than that reported in an IR study[23] (1973 cm^{-1}, in D_2O), but this difference may be attributed to the broad width of the line. The frequencies for the Fe–CO and C–O stretching modes are typical of those seen in CO-bound heme proteins and porphyrins. For example, heme systems in which the fifth ligand is a neutral imidazole display Fe–CO stretching modes in the 490–525-cm^{-1} region and C–O stretching modes in the 1940–1980-cm^{-1} region.[37] In addition to being sensitive to the ligand occupying the fifth coordination position, the frequencies of these modes are affected by π-back-bonding from the iron porphyrin and by steric interactions between the bound CO and its local environment. The similarity of the Fe–CO and C–O stretching frequencies to those of heme proteins suggests that the electronic structure of iron coordination in Fe–BLM is similar to that in a porphyrin macrocycle.

Implications for Bleomycin Chemistry. The amide group is known to chelate metal ions. Coordination can occur at either the oxygen or nitrogen atom.[38] The observed line at 1608 cm^{-1} confirms the coordination of the nitrogen atom of the β-hydroxyhistidine amide. Two resonance forms are possible for a deprotonated amide bound to a metal ion through the nitrogen atom:

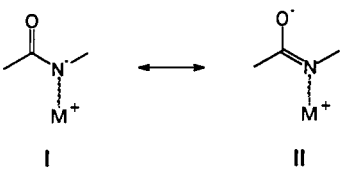

I II

In resonance form II, the C–O bond is lengthened and the C–N bond is shortened relative to form I. Thus, the shift of the amide carbonyl vibrations to lower frequency induced by coordination to a metal ion has been attributed to an increased contribution of resonance form II.[39] The relatively low frequency of the amide C–O stretching mode in Fe–BLM is consistent with coordination of the β-hydroxyhistidinyl amide nitrogen and the concomitant increases contribution of form II. In addition, the present Raman data show a further low-frequency shift (1608 to 1595 cm^{-1}) of this line induced by reduction of iron. This is an expected result, as the increased electron density of ferrous iron would favor form II, whereas the ferric complex would favor the negatively charged

(33) Several weak lines in the 750–800-cm^{-1} region also show D_2O shifts, but these are contributions from nonresonance-enhanced modes. Similarly, the broadness of the 554-cm^{-1} peak in the D_2O spectrum is due to overlap with such modes.

(34) Nakagawa, I.; Shimanouchi, T. *Spectrochim. Acta* **1964**, *20*, 429–439.

(35) Sitter, A. J.; Shifflett, J. R.; Terner, J. *J. Biol. Chem.* **1988**, *263*, 13032–13038.

(36) Takahashi, S.; Rousseau, D. L. Manuscript in preparation.

(37) Yu, N. T.; Kerr, E. A. In *Biological Applications of Raman Spectroscopy*; Spiro, T. G., Ed.; Wiley & Sons: New York, 1988; Vol. 3, pp 39–95.

(38) Sigel, H.; Martin, R. B. *Chem. Rev.* **1982**, *82*, 385–426.

(39) Kim, M. K.; Martell, A. E. *Biochemistry* **1964**, *3*, 1169–1174.

nitrogen of form I. A similar mechanism was proposed by Guajardo et al. in their explanation of the IR spectra of Fe–PMA.[29] Interestingly, the frequency of this line in the spectrum of CO–Fe(II)–BLM (1607 cm^{-1}) is comparable to that of the ferric complex (1608 cm^{-1}). This shift pattern is reminiscent of the electron density marker lines in iron porphyrins. For example, the ν_4 line in iron porphyrins typically appears at 1370, 1350, and 1370 cm^{-1} for the ferric, ferrous, and carbon monoxy forms, respectively,[40] and is an indicator of the π-electron density of the macrocycle, which is in turn affected by the d_π electron density of the iron atom. In these systems, the π^* orbital of bound carbon monoxide is electron withdrawing, making the electron density of the ferrous iron similar to that of the ferric state, resulting in the shift of the ν_4 line to higher frequency. Thus, we propose that the frequency shift pattern of the 1608-cm^{-1} line can be explained by the same mechanism. This is further supported by the CO stretching vibration, which is lowered relative to that of free CO due to the increased occupancy of the π^* antibonding orbital, and by the optical spectrum of CO–Fe(II)–BLM, which is similar to that of Fe(III)–BLM (Figure 2). It should be pointed out that the β-hydroxyhistidinyl amide is conjugated to the pyrimidine ring and one can speculate that together they comprise a delocalized π-electron buffer similar in function to the electron-buffering capabilities of the porphyrin macrocycle:[41]

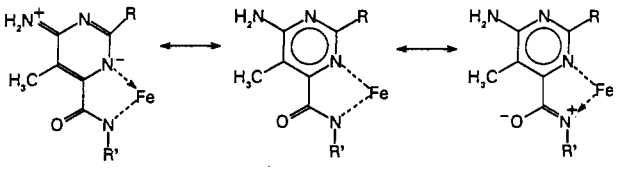

This hypothesis is especially intriguing when one considers the elegant synthetic studies of Ohno and co-workers,[42–44] who have shown with a series of PYML[45] analogs of BLM that by increasing the electron-donating ability of the pyrimidine ring (which has been replaced with substituted pyridines in their PYML series) the ability to activate oxygen is increased. Thus, the delocalized system which we propose may partially explain the similar spectroscopic characteristics and reactivity of iron–bleomycin and heme proteins.

(40) Spiro, T. G.; Li, X.-Y. In *Biological Applications of Raman Spectroscopy*; Spiro, T. G., Ed.; Wiley & Sons: New York, 1988; Vol. 3, pp 1–37.

(41) Molecular orbital calculations of the iron porphyrin system demonstrate that the porphyrin macrocycle donates and withdraws electrons to the ferric and from the ferrous iron atom, respectively, to make the electron density on the iron invariant: Zerner, M.; Gouterman, M.; Kobayashi, H. *Theor. Chim. Acta* **1966**, *6*, 363–400.

(42) Kittaka, A.; Sugano, Y.; Otsuka, M.; Ohno, M.; Sugiura, Y.; Umezawa, H. *Tetrahedron Lett.* **1986**, *27*, 3631–3634.

(43) Sugano, Y.; Kittaka, A.; Otsuka, M.; Ohno, M.; Sugiura, Y.; Umezawa, H. *Tetrahedron Lett.* **1986**, *27*, 3635–3638.

(44) Owa, T.; Haupt, A.; Otsuka, M.; Kobayashi, S.; Tomioka, N.; Itai, A.; Ohno, M.; Shiraki, T.; Uesugi, M.; Sugiura, Y.; Maeda, K. *Tetrahedron* **1992**, *48*, 1193–1208.

(45) PYML is the common abbreviation for a family of *N*-[(6-{[((*S*)-2-amino-2-carbamoylethyl)amino]methyl}-2-pyridyl)carbonyl]-L-histidines.